A UNITARY ESPRIT ALGORITHM FOR CARRIER FREQUENCY OFFSET ESTIMATION

Tadeu N. Ferreira[1,2]

[1]Telecommunications Department
Federal Fluminense University (UFF)
Rua Passo da Pátria, 156, Bl. D, Sala 500
24210-240, Niterói, RJ, Brazil
tadeu.n.ferreira@gmail.com

Sergio L. Netto[2], *Paulo S. R. Diniz*[2]

[2]Electrical Engineering Program/COPPE/Poli
Federal University of Rio de Janeiro
P.O. Box 68504,
21941-972 Rio de Janeiro, RJ, Brazil
{sergioln, diniz}@lps.ufrj.br

ABSTRACT

This article presents a low-complexity parametric algorithm for the estimation of the carrier frequency offset (CFO) in orthogonal frequency division multiplexing systems. The proposed algorithm is equivalent to the Unitary ESPRIT algorithm, originally devised for estimating the direction-of-arrival of a wavefront, now applied to the CFO scenario. It is verified that the proposed algorithm reduces the overall computational complexity in around 40%, while sustaining the error-rate performance achieved by the standard ESPRIT algorithm.

Index Terms— Direction of arrival estimation, Parameter estimation, Array signal processing.

I. INTRODUCTION

Modern communication applications have progressively required higher data rates [1] which tend to increase the intersymbol interference (ISI), severely degrading the receiver performance. A possible approach to ISI mitigation emerged from the development of orthogonal frequency division multiplexing (OFDM), which has been incorporated to several communications standards [2].

A general scheme for the OFDM system is presented in Fig. 1. The use of the discrete Fourier transform (DFT) in the receiver and the inverse DFT (IDFT) in the transmitter provides the orthogonality for the carriers, which is the key for a proper ISI mitigation. However, the presence of some phase noise or any asynchronism among the modulators and demodulators may generate carrier frequency offset (CFO) [3], destroying the subchannel orthogonality and affecting the overall system performance. In order to restore the carrier orthogonality, the CFO must be properly compensated.

Among the existing methods for CFO estimation, some parametric algorithms have been adapted to the OFDM framework, such as the standard ESPRIT algorithm [4] or the covariance-based (CB) scheme [5]. In this article, a new version for ESPRIT is proposed requiring real-only operations [6] [7], thus reducing even further the associated computational complexity. To introduce the Unitary ESPRIT for CFO estimation, this paper is organized as follows: In Section II we present a general OFDM model including a possible CFO interference. Section III describes the proposed Unitary ESPRIT algorithm for CFO estimation. Comparisons between the Standard and Unitary ESPRIT versions are performed in Section IV, in terms of computational complexity, and in Section V, for the mean squared error (MSE) metrics. Section VI presents some concluding remarks for the proposed algorithm.

This work was partially supported by the Brazilian councils for research CNPq and FAPERJ.

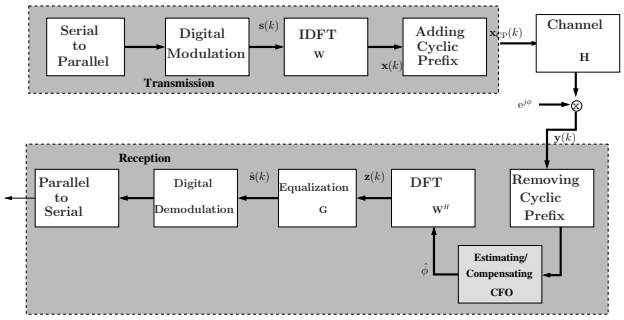

Fig. 1. OFDM system with estimated and compensated CFO.

II. ESPRIT ALGORITHM FOR CFO ESTIMATION

II-A. General Modeling

Consider an OFDM system represented in Fig. 1, where data is grouped into length-P blocks by a serial-to-parallel converter. Afterwards, length-P vectors $\mathbf{s}(k)$ of symbols are generated and associated to different carriers by the modulation process. Some of the carriers, the so-called *virtual carriers*, are not effectively used, but they are necessary for the estimation process. Hence, $\mathbf{s}(k)$ is transformed onto the time-domain length-P vector $\mathbf{x}(k)$ through the operation

$$\mathbf{x}(k) = \mathbf{W}_P \mathbf{s}(k), \tag{1}$$

where $\mathbf{W}_P$ is a $P \times P$ submatrix of an $N \times N$ IDFT matrix containing the entries with no relation to the virtual carriers.

Transmission is performed on a channel represented by an FIR filter $\mathbf{h}$, with length L, by a linear convolution between $\mathbf{x}(k)$ and $\mathbf{h}$. Consider that $\mathbf{x}_{\text{CP}}(k)$ is a version of $\mathbf{x}(k)$

with a cyclic-prefix (CP) insertion [3]. Therefore, the linear convolution between $\mathbf{x}_{\text{CP}}(k)$ and $\mathbf{h}$ becomes equivalent to the operation $\mathbf{H}_P\mathbf{x}(k)$, where $\mathbf{H}_P$ is a $P \times P$ submatrix of the circulant matrix $\mathbf{H}_N$, containing the entries related to the non-virtual carriers. Moreover $\mathbf{H}_N$ is an $N\times N$ circulant matrix, whose first column is $\mathbf{h}$ followed by $(N-L)$ zeros.

The receiver applies the DFT reduced $\mathbf{W}_P^{\text{H}}$ matrix, such that

$$\mathbf{W}_P^{\text{H}}\mathbf{H}_P\mathbf{W}_P = \mathbf{\Lambda}_P \tag{2}$$

making the transmission process equivalent to the eigendecomposition of the circulant matrix $\mathbf{H}_P$, where $\mathbf{W}_P$ consists of a unitary set of eigenvectors and the $P\times P$ diagonal matrix $\mathbf{\Lambda}_P$ [8].

Therefore, the convolution of vectors $\mathbf{x}(k)$ and $\mathbf{h}$ is equivalent to the multiplication $\mathbf{\Lambda}_P\mathbf{s}(k)$. Since $\mathbf{\Lambda}_P$ is diagonal, there is no interference among the samples of $\mathbf{s}(k)$ in the transmission, which corresponds to zero ISI and allows a simpler symbol recovery. In fact, we may express $\mathbf{z}(k)$, obtained after CP removal and the DFT as

$$\mathbf{z}(k) = \mathbf{\Lambda}_P\mathbf{s}(k). \tag{3}$$

From eq. (3), the $P\times 1$ time-domain received signal $\mathbf{y}(k)$ may be written as

$$\mathbf{y}(k) = \mathbf{W}_P\mathbf{\Lambda}_P\mathbf{s}(k). \tag{4}$$

In a system which is immune to both additive white Gaussian noise (AWGN) and CFO, $\mathbf{s}(k)$ may be easily recovered from eq. (3) by a linear equalizer $\mathbf{G} = \mathbf{\Lambda}_P^{-1}$, that is,

$$\hat{\mathbf{s}}(k) = \mathbf{G}\mathbf{z}(k) = \mathbf{\Lambda}_P^{-1}\mathbf{\Lambda}_P\mathbf{s}(k). \tag{5}$$

II-B. CFO Modeling and Estimation

Assume that due to some phase offset ϕ between carrier oscillators on both the transmitter and the receiver, there is a CFO interference on the transmitted symbols. Such interference is modeled as deterministic, unknown at the receiver side and cumulative along both the carriers and the data blocks. If the system is still modeled without AWGN, eq. (4) becomes [4]

$$\mathbf{y}(k) = \mathbf{E}\mathbf{W}_P\mathbf{\Lambda}_P\mathbf{s}(k)\delta(k,\phi), \tag{6}$$

where matrix $\mathbf{E} = \text{diag}(1, \text{e}^{j\phi}, \text{e}^{j2\phi}, \ldots, \text{e}^{j(P-1)\phi})$ models the CFO influence on each carrier and $\delta(k,\phi) = \text{e}^{j(k-1)\phi(N+L)}$ models the CFO inside a specific block. Hence, after equalization, the estimated signal becomes

$$\hat{\mathbf{s}}(k) = \mathbf{G}\mathbf{W}_P^{\text{H}}\mathbf{E}\mathbf{\Lambda}_P\mathbf{W}_P\mathbf{s}(k)\delta(k,\phi), \tag{7}$$

indicating that the IDFT and DFT terms do not cancel each other any longer due to some loss in the carrier orthogonality, which may be restored by an appropriate CFO compensation.

The ESPRIT approach to perform estimation exploits some redundancies inherent to the transmission model [4] [9]. Consider the $(M+1)\times$1-auxiliary forward and backward window vectors

$$\mathbf{y}_F^{(i)}(k) = \begin{bmatrix} y_{i-1}(k) & y_i(k) & \ldots & y_{i+M-1}(k)\end{bmatrix}^{\text{T}}, \tag{8}$$

$$\mathbf{y}_B^{(i)}(k) = \begin{bmatrix} y_{N-i}(k) & y_{N-i-1}(k) & \ldots & y_{N-i-M}(k)\end{bmatrix}^{\text{T}}, \tag{9}$$

for $i = 1, 2, \ldots, (N-M)$, and $N > M \geq P$, where $y_i(k)$ is the i^{th} entry of $\mathbf{y}(k)$. We also define $\mathbf{E}_{M+1}$, containing the first $(M+1)$ lines and columns of $\mathbf{E}$, and the diagonal matrix

$$\mathbf{\Delta} = \text{diag}(1, \text{e}^{j\phi}, \text{e}^{j\phi+2\pi/M}, \ldots, \text{e}^{j\phi+2\pi(P-1)/M}). \tag{10}$$

We may then write

$$\mathbf{y}_F^{(i)}(k) = \mathbf{A}\mathbf{\Delta}^i\tilde{\mathbf{s}}(k); \quad \mathbf{y}_B^{(i)}(k) = \mathbf{A}\mathbf{\Delta}^i\mathbf{r}(k), \tag{11}$$

where $\mathbf{A} = \mathbf{E}_{M+1}\mathbf{W}_{M+1}$ and

$$\tilde{\mathbf{s}}(k) = \text{e}^{j(k-1)\phi(N+L)}\mathbf{\Lambda}_P\mathbf{s}(k), \tag{12}$$

$$\mathbf{r}(k) = \text{e}^{-j\phi(N-1)}\text{diag}(1, \text{e}^{j2(N-1)\pi/M}, \text{e}^{j4(N-1)\pi/M}, \ldots, \text{e}^{j2(P-1)\pi/M})\tilde{\mathbf{s}}^*(k), \tag{13}$$

with a superscript * denoting the complex-conjugate operation.

An $(M+1)\times(M+1)$ forwards-backwards estimation covariance matrix $\mathbf{Y}_E^{(i)}$ is given by

$$\mathbf{Y}_E^{(i)} = \mathbf{y}_F^{(i)}(k)\left(\mathbf{y}_F^{(i)}(k)\right)^{\text{H}} + \mathbf{y}_B^{(i)}(k)\left(\mathbf{y}_B^{(i)}(k)\right)^{\text{H}}. \tag{14}$$

By averaging $\mathbf{Y}_E^{(i)}$ along the variable i, we get

$$\begin{aligned}\mathbf{R}_Y &= \frac{1}{K(N-M)}\sum_{k=1}^{K}\sum_{i=1}^{(N-M)}\mathbf{Y}_E^{(i)}(k)\\ &= \mathbf{A}\sum_{k=1}^{K}\sum_{i=1}^{(N-M)}\left(\tilde{\mathbf{s}}(k)(\tilde{\mathbf{s}}(k))^{\text{H}} + \mathbf{r}(k)(\mathbf{r}(k))^{\text{H}}\right)\mathbf{A}^{\text{H}}\\ &= \mathbf{A}\mathbf{R}_{\tilde{\mathbf{s}}}\mathbf{A}^{\text{H}}.\end{aligned} \tag{15}$$

In the presence of AWGN of power σ_N^2, both $\mathbf{y}_F^{(i)}(k)$ and $\mathbf{y}_B^{(i)}(k)$ become contaminated by a vectorial AWGN, which changes the covariance model above to

$$\mathbf{R}_Y = \mathbf{A}\mathbf{R}_{\tilde{\mathbf{s}}}\mathbf{A}^{\text{H}} + \sigma_N^2\mathbf{I}. \tag{16}$$

This relationship has a very similar structure to the covariance model for the DoA estimation in sensor arrays [10]. Hence, as in the ESPRIT algorithm for DoA estimation, an eigendecomposition can be performed on $\mathbf{R}_Y$, yielding

$$\mathbf{R}_Y = \mathbf{U}\mathbf{\Sigma}^2\mathbf{U}^{\text{H}}. \tag{17}$$

The P largest eigenvalues belong to the signal subspace and may form the diagonal matrix $\mathbf{\Sigma}_s^2$, with the associated eigenvectors constituting the columns of $\mathbf{U}_s$. In eq. (16), the term $\mathbf{A}\mathbf{R}_{\tilde{\mathbf{s}}}\mathbf{A}^{\text{H}}$ is the only responsible for the signal subspace. Hence, there must be a full-rank transformation $\mathbf{T}$ such that

$$\mathbf{A} = \mathbf{U}_s\mathbf{T}. \tag{18}$$

Consider the $M\times(M+1)$ selection matrices, $\mathbf{J}_0 = \begin{bmatrix}\mathbf{I}_M & \mathbf{0}\end{bmatrix}$ and $\mathbf{J}_1 = \begin{bmatrix}\mathbf{0} & \mathbf{I}_M\end{bmatrix}$, where $\mathbf{I}_M$ is an $M\times M$ identity matrix and $\mathbf{0}$ is an $M\times 1$ vector of zeros. As shown in [4], matrix $\mathbf{A}$ presents the invariance property $\mathbf{J}_0\mathbf{A}\mathbf{\Delta} = \mathbf{J}_1\mathbf{A}$, such that

$$\mathbf{J}_0\mathbf{U}_s\mathbf{\Psi} = \mathbf{J}_1\mathbf{U}_s, \tag{19}$$

where

$$\mathbf{\Psi} = \mathbf{T}\mathbf{\Delta}\mathbf{T}^{-1}. \tag{20}$$

Due to the AWGN component and to finite representation issues, eq. (19) does not have an accurate solution and a total least-squares (TLS) algorithm [4] may be used to obtain the estimate $\hat{\mathbf{\Psi}}$. One can then determine $\mathbf{\Delta}$ by using eq. (20), and the CFO parameter ϕ may be estimated as

$$\hat{\phi} = \frac{1}{j} \ln \frac{\mathrm{tr}(\mathbf{\Delta})}{\sum_{k=0}^{P-1} \mathrm{e}^{jk\omega}}. \tag{21}$$

III. UNITARY ESPRIT

III-A. New Structures and Modeling

In the DoA framework, the Unitary ESPRIT algorithm imposes an additional centro-Hermitian (CH) constraint on the receiving-array geometry: antennas which are symmetric in relation to the array centroid must present similar characteristics. In an OFDM system, adjacent IDFT/DFT carriers automatically obey both the CH as well as the original rotational invariance constraints. When using virtual carriers, however, one must guarantee that these additional carriers must be symmetrically chosen in the transmitted set. For example, if the first carrier is chosen to be virtual, the last one (that is, the N^{th} one) must also be virtual.

Consider the rotational matrix $\mathbf{Q}_a$ defined as

$$\mathbf{Q}_a = \frac{1}{\sqrt{2}} \begin{bmatrix} \mathbf{I}_{a/2} & j\mathbf{I}_{a/2} \\ \mathbf{\Pi}_{a/2} & -j\mathbf{\Pi}_{a/2} \end{bmatrix}, \tag{22}$$

where $\mathbf{\Pi}_i$ is an $i \times i$ permutation matrix with 1 in its antidiagonal and zeros in the other elements. We may define the following transformations on an $a \times a$ matrix $\mathbf{M}$:

$$\psi(\mathbf{M}) = \mathbf{Q}_a^{\mathrm{H}} \mathbf{M} \mathbf{Q}_a, \tag{23}$$

$$\mathcal{E}(\mathbf{M}) = \begin{bmatrix} \mathbf{M} & \mathbf{\Pi}_a \mathbf{M}^* \mathbf{\Pi}_a \end{bmatrix}. \tag{24}$$

In [6], it is shown that the composite of $\mathcal{T}(\mathbf{M}) = \psi(\mathcal{E}(\mathbf{M}))$ over a complex CH matrix generates a real matrix. This is the basis for the Unitary ESPRIT presented below for the OFDM setup, which also uses the selection matrices

$$\mathbf{K}_0 = \mathbf{Q}_M^{\mathrm{H}} (\mathbf{J}_0 + \mathbf{\Pi}_M \mathbf{J}_0 \mathbf{\Pi}_{M+1}) \mathbf{Q}_{M+1}, \tag{25}$$

$$\mathbf{K}_1 = j\mathbf{Q}_M^{\mathrm{H}} (\mathbf{J}_0 - \mathbf{\Pi}_M \mathbf{J}_0 \mathbf{\Pi}_{M+1}) \mathbf{Q}_{M+1}, \tag{26}$$

where $\mathbf{K}_0$ and $\mathbf{K}_1$ play similar roles to $\mathbf{J}_0$ and $\mathbf{J}_1$ defined above.

III-B. CFO Estimation with Real Structures

Consider the transformation $\mathcal{T}(\cdot)$ is applied to the general data structure $\mathbf{R}_Y$, defined in eq. (15). A covariance matrix for $\mathbf{Y}_E$ is given by $\mathbf{R}_{\mathcal{T}} = \mathcal{T}(\mathbf{R}_Y)\mathcal{T}^{\mathrm{H}}(\mathbf{R}_Y)$, whose eigendecomposition leads to

$$\mathbf{R}_{\mathcal{T}} = \mathbf{U}\mathbf{\Sigma}^2\mathbf{U}^{\mathrm{H}}. \tag{27}$$

The P largest eigenvalues belong to the signal subspace and are grouped in the diagonal matrix $\mathbf{\Sigma}_s^2$, whereas the associated eigenvectors form the $(M+1) \times P$ matrix $\mathbf{U}_s$.

As in the algorithm presented in Section II, two transformations $\mathbf{U}_0 = \mathbf{K}_0\mathbf{U}_s$ and $\mathbf{U}_1 = \mathbf{K}_1\mathbf{U}_s$ are applied on matrix $\mathbf{U}_s$, giving rise to the invariance relation $\mathbf{U}_1 = \mathbf{U}_0\mathbf{\Upsilon}$, which can be solved by a TLS algorithm. In this case, consider the auxiliary structure

$$\mathbf{U}_{\text{TLS}} = \begin{bmatrix} \mathbf{U}_0^{\mathrm{H}} \\ \mathbf{U}_1^{\mathrm{H}} \end{bmatrix} \begin{bmatrix} \mathbf{U}_0 & \mathbf{U}_1 \end{bmatrix}, \tag{28}$$

whose eigendecomposition may be written as

$$\mathbf{U}_{\text{TLS}} = \mathbf{E}_{\text{TLS}} \mathbf{\Lambda}_{\text{TLS}} \mathbf{E}_{\text{TLS}}^{\mathrm{H}}. \tag{29}$$

By dividing $\mathbf{E}_{\text{TLS}}$ into 4 submatrices,

$$\mathbf{E}_{\text{TLS}} = \begin{bmatrix} \mathbf{E}_{00} & \mathbf{E}_{01} \\ \mathbf{E}_{10} & \mathbf{E}_{11} \end{bmatrix}, \tag{30}$$

the TLS estimation for $\mathbf{\Upsilon}$ can be obtained as $\hat{\mathbf{\Upsilon}} = -\mathbf{E}_{01}\mathbf{E}_{11}^{-1}$. The eigendecomposition of $\hat{\mathbf{\Upsilon}}$, $\hat{\mathbf{\Upsilon}} = \mathbf{T}\mathbf{\Omega}\mathbf{T}^{-1}$, determines the diagonal matrix $\mathbf{\Omega}$ which is related to the parameters of the original complex solution by [6]:

$$\hat{\mathbf{\Phi}} = -(\mathbf{\Omega} - j\mathbf{I}_M)(\mathbf{\Omega} + j\mathbf{I}_M)^{-1}. \tag{31}$$

IV. COMPUTATIONAL COMPLEXITY

Table I includes the complexity of some operations involving real or complex matrices, using a real flop as basic unit. These results allow a better comparison of the computational complexity of the Standard and Unitary ESPRIT algorithms for CFO estimation, which are summarized in Table II.

Table I. Real flops required by some matricial operations.

Operation	Real [8]	Complex
Non-Hermitian EVD	$\mathcal{O}(25n^3)$	$\mathcal{O}(25n^3)$
Hermitian EVD	$\mathcal{O}(n^2)$	$\mathcal{O}(2n^2)$
Full Inversion	$\mathcal{O}(2n^3/3)$	$\mathcal{O}(8n^3/3)$
Multiplication	$\mathcal{O}(n^3)$	$\mathcal{O}(4n^3)$

The computational complexity of each algorithm, considering all operations required, is provided in Table III, already taking into account information from Table I.

From Table III, one notices that the computational complexity for the Unitary ESPRIT algorithm is lower than the complexity for the Standard ESPRIT. For the 3rd generation long-term-evolution (3G-LTE) parameters, for instance, where $P = 310$ and $M = 512$, there is a reduction of around 40% in the amount of real flops when Unitary ESPRIT is used instead of the Standard ESPRIT.

V. COMPUTER SIMULATIONS

The performance of both algorithms analyzed in Section IV, can be assessed with the normalized mean-squared error (NMSE) metrics defined as [4]:

$$\text{NMSE} = \frac{1}{Q} \sum_{i=1}^{Q} \left(\frac{\hat{\theta} - \theta}{2\pi/N} \right)^2, \tag{32}$$

where Q denotes the amount of Monte Carlo runs used for simulating an ensemble averaging.

Table II. Summary of Standard [4] and Unitary ESPRIT algorithms for CFO estimation: [C] indicates complex operations.

Standard ESPRIT	Unitary ESPRIT
$[\mathbf{U}_s, \mathbf{\Lambda}_s] = \text{EVD}\left(\hat{\mathbf{R}}\right)$	$\mathbf{Y}_E = \sum(\mathbf{y}_B + \mathbf{y}_F)$ [C]
$\mathbf{E}_0 = \mathbf{J}_0\mathbf{U}_s$	$\mathbf{R}_{\mathcal{T}} = \mathcal{T}(\mathbf{R}_Y)\mathcal{T}^{\text{H}}(\mathbf{R}_Y)$ [C]
$\mathbf{E}_1 = \mathbf{J}_1\mathbf{U}_s$	$\mathbf{\Xi} = \mathbf{\Pi}_M\mathbf{J}_0\mathbf{\Pi}_{M+1}$
$\mathbf{E}_a = \begin{bmatrix}\mathbf{E}_0^{\text{H}} \\ \mathbf{E}_1^{\text{H}}\end{bmatrix}[\mathbf{E}_0 \quad \mathbf{E}_1]$	$\mathbf{K}_0 = \mathbf{Q}_{M+1}^{\text{H}}(\mathbf{J}_0 + \mathbf{\Xi})\mathbf{Q}_{2(M+1)}$
$[\mathbf{E}, \mathbf{\Lambda}] = \text{EVD}(\mathbf{E}_a)$	$\mathbf{K}_1 = j\mathbf{Q}_{M+1}^{\text{H}}(\mathbf{J}_0 - \mathbf{\Xi})\mathbf{Q}_{2(M+1)}$
$\mathbf{E} = \begin{bmatrix}\mathbf{E}_{00} & \mathbf{E}_{01} \\ \mathbf{E}_{10} & \mathbf{E}_{11}\end{bmatrix}$	$[\mathbf{U}_s, \mathbf{\Lambda}_s] = \text{EVD}\left(\hat{\mathbf{R}}_{\mathcal{T}}\right)$
$\mathbf{\Psi} = -\mathbf{E}_{01}\mathbf{E}_{11}^{-1}$	$\mathbf{U}_0 = \mathbf{K}_0\mathbf{U}_s; \ \mathbf{U}_1 = \mathbf{K}_1\mathbf{U}_s$
$[\mathbf{T}, \hat{\mathbf{\Delta}}] = \text{EVD}(\mathbf{\Psi})$	$\mathbf{E}_a = \begin{bmatrix}\mathbf{U}_0^{\text{H}} \\ \mathbf{U}_1^{\text{H}}\end{bmatrix}[\mathbf{U}_0 \quad \mathbf{U}_1]$
	$[\mathbf{E}, \mathbf{\Lambda}] = \text{EVD}(\mathbf{E}_a)$
	$\mathbf{E} = \begin{bmatrix}\mathbf{E}_{00} & \mathbf{E}_{01} \\ \mathbf{E}_{10} & \mathbf{E}_{11}\end{bmatrix}$
	$\mathbf{\Upsilon} = -\mathbf{E}_{01}\mathbf{E}_{11}^{-1}$
	$[\mathbf{T}, \mathbf{\Omega}] = \text{EVD}(\mathbf{\Upsilon})$
	$\hat{\mathbf{\Delta}} = -(\mathbf{\Omega} - j\mathbf{I}_M)(\mathbf{\Omega} + j\mathbf{I}_M)^{-1}$ [C]

Table III. Computational complexity associated to the Standard and Unitary ESPRIT algorithms for CFO estimation.

Operation [8]	**Standard**		**Unitary**	
	#	Real Flops	#	Real Flops
Non-Herm. EVD	1	$25P^3$	1	$25P^3$
Hermitian EVD	2	$8P^2+2(M+1)^2$	1	$4P^2+2(M+1)^2$
Inverse	1	$8M^3/3$	2	$4M^3/3$
Real Multiplic.	–		9	$4P^2(M+1)+2P^3$
Cplx. Multiplic.	5	$16P^2M+4P^3$	1	$8(M+1)^3$
Dominant Terms	–	$29P^3+2.7M^3+$ $15P^2M$	–	$27P^3+1.3M^3+$ $4P^2(M+1)$

In this paper, the simulations were based on the 3G-LTE standard for mobile phones [11], characterized by $N = 512$ carriers, where $P = 310$ of them are non-virtual. The input symbols were randomly generated over $Q = 200$ independent runs and we used a data block of length $M = 511$. The simulated fading channels were extracted from [11] using both rural (modeled with $L = 11$ taps) and urban ($L = 55$ taps) channel models. The CFO was modeled as a deviation of $0.2\pi/N$ in the carrier frequency.

Fig. 2 shows the results of simulations for the aforementioned scenario with different SNR levels. In this case, the NMSE metrics for both algorithms were quite comparable, with a slight advantage for the Unitary ESPRIT, which also requires 40% less computational burden, as given in Section IV. These results are similar to the ones often found in DoA measurements or alternative CFO scenarios.

VI. CONCLUSIONS

A unitary version of the ESPRIT algorithm was introduced for CFO estimation. The proposed algorithm represents a significant reduction in the amount of computer operations

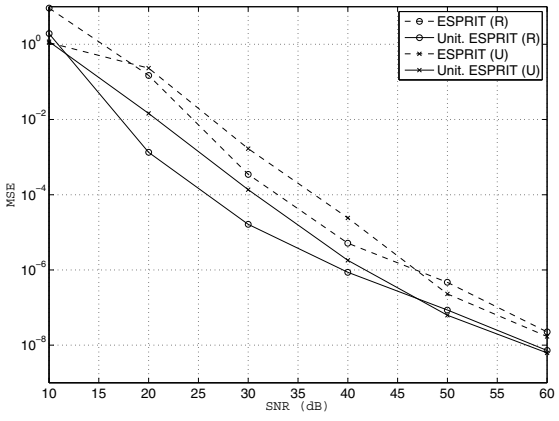

Fig. 2. NMSE for Standard TLS-ESPRIT and Unitary ESPRIT for both rural (R) and urban (U) channel models.

(around 40%, in the simulated scenarios), with a similar NMSE performance, when compared to a standard approach.

VII. REFERENCES

[1] A. Vahlin and N. Holte, "OFDM for broadcasting in presence of analogue co-channel interference," *IEEE Trans. Broadcasting*, vol. 41, no. 3, pp. 89–93, Sept. 1995.

[2] H. Rohling, T. May, K. Bruninghaus, and R. Grunheid, "Broad-band OFDM radio transmissions for multimedia applications," *Proc. IEEE*, vol. 87, no. 10, pp. 1778–1789, Oct. 1999.

[3] T. Pollet, M. Van Bladel, and M. Moeneclaey, "BER sensitivity of OFDM systems to carrier frequency offset and Wiener phase noise," *IEEE Trans. Communications*, vol. 43, no. 2, pp. 191–193, Feb. 1995.

[4] U. Tureli, H. Liu, and M. Zoltowski, "OFDM blind carrier offset estimation: ESPRIT," *IEEE Trans. Communications*, vol. 48, no. 9, pp. 1459–1461, Sept. 2000.

[5] T. N. Ferreira, S. L. Netto, P. S. R. Diniz, L. G. Baltar, and J. A. Nossek, "Low complexity blind estimation of the carrier frequency offset in multicarrier systems," in *Proc. IEEE Int. Conf. Acoustics, Speech, Signal Processing*, Las Vegas, USA, Apr. 2008, pp. 3045–3048.

[6] M. Haardt and J. A. Nossek, "Unitary ESPRIT: How to obtain increased estimation accuracy with a reduced computational burden," *IEEE Trans. Acoust., Speech, Signal Processing*, vol. 43, no. 5, pp. 1232–1242, May 2005.

[7] T. N. Ferreira, S. L. Netto, and P. S. R. Diniz, "Covariance-based direction-of-arrival estimation with real structures," *IEEE Signal Processing Letters*, vol. 15, pp. 757–760, Dec. 2008.

[8] G. Golub and C. V. Loan, *Matrix Computations*, 3rd ed. New York: Johns Hopkins Univ. Press, 1996.

[9] M. Zatman, "Subspace domain forwards-backwards averaging," in *Proc. IEEE Int. Conf. Acoustics, Speech, Signal Processing*, Seattle, USA, Apr. 1998, pp. 1945–1948.

[10] R. Roy and T. Kailath, "ESPRIT - estimation of parameters via rotational invariance techniques," *IEEE Trans. Acoust., Speech, Signal Processing*, vol. 37, no. 7, pp. 984–995, July 1989.

[11] 3GPP GERAN: Radio transmission and reception, "3GPP TS 45.005 v7.8.0," 3rd Generation Partnership Project, Tech. Rep., Dec. 2006.